Eur. Phys. J. A **31**, 397–402 (2007)
DOI 10.1140/epja/i2006-10170-1

THE EUROPEAN PHYSICAL JOURNAL A

Special Article – QNP 2006

Modern theory of nuclear forces A.D. 2006

U.-G. Meißner[a]

HISKP (Th), Universität Bonn, D-53115 Bonn, Germany and
IKP, FZ Jülich, D-52425 Jülich, Germany

Received: 24 September 2006
Published online: 16 February 2007 –

Abstract. I present and discuss recent results on nuclear forces and few-nucleon systems obtained in the framework of chiral effective nuclear field theory.

PACS. 13.75.Gx Pion-baryon interactions – 25.30.Rw Electroproduction reactions – 12.39.Fe Chiral Lagrangians

1 Introduction

One of the most challenging problems of strong QCD is the derivation of nuclear forces. The underlying QCD fields, quarks and gluons, are confined within hadrons, therefore nuclear forces are the residual forces between colorless objects, much like the van der Waals forces in molecular physics. Furthermore, typical energy scales in nuclear physics correspond to a low-resolution microscope, *e.g.* producing a neutral pion at threshold by a real photon requires a photon laboratory energy of about 150 MeV. Stated differently, nuclei are made of protons and neutrons plus virtual mesons —their QCD substructure is effectively masked. Since the nuclear binding energies are much smaller than the nuclear masses, we essentially have to deal with a non-relativistic problem. It appears thus appropriate to analyze the nuclear A-body problem by solving the Schrödinger equation

$$H\Psi_A = E_A\Psi_A\,, \qquad H = T + V = \sum_A \frac{p_A^2}{2m_{\rm N}} + V\,, \quad (1)$$

where the potential V is a string of terms, $V = V_{\rm NN} + V_{\rm 3N} + V_{\rm 4N} + \ldots$. Traditionally, the two-nucleon potential $V_{\rm NN}$ is reconstructed from the large body of pp and np scattering data to a high accuracy. However, the two-nucleon forces alone do not give the proper nuclear binding energies and level schemes —a small three-nucleon force (TNF) is needed to cure this problem. Making an ansatz for such a TNF with a few adjustable parameters, the pattern of binding energies and excited states for nuclei up to $A \simeq 12$ based on *ab initio* Monte Carlo simulations is amazingly well described (for a recent status report, see *e.g.* [1]). However, there are important open problems: 1) Why is there this hierarchy $V_{\rm 2N} \gg V_{\rm 3N} \gg V_{\rm 4N}$? 2) Gauge and chiral symmetries are difficult to include and 3) what is the connection to QCD? As will be discussed in what follows, chiral effective field theory (EFT) offers an approach that a) is linked to QCD via its symmetries; b) allows for systematic calculations with a controlled theoretical error; c) explains the observed hierarchy of the nuclear forces and gives consistent two-, three-, and four-body forces; d) matches nucleon structure to nuclear dynamics; e) offers the possibility of a consistent inclusion of strange quarks (hyper-nuclear physics); f) allows for a lattice formulation/chiral extrapolations; and g) puts nuclear physics on a sound basis.

2 Effective field theory for nuclear forces

In this section, I briefly discuss the formulation of the EFT for few-baryon interactions (NN, NNN, YN, ...). As discussed before, the underlying fields are ground-state baryons and the octet of Goldstone bosons of QCD. The starting point is the chiral effective Lagrangian (for the moment, I restrict myself to the two-flavor case of pions and nucleons),

$$\mathcal{L}_{\rm EFF} = \mathcal{L}_{\pi\pi} + \mathcal{L}_{\pi{\rm N}} + \mathcal{L}_{\rm NN} + \ldots\,, \quad (2)$$

which allows for a systematic expansion in powers of Q/Λ_χ and M_π/Λ_χ, where Q denotes any external soft scale, M_π is the pion mass related to explicit chiral symmetry breaking and $\Lambda_\chi \simeq 1\,{\rm GeV}$ is the hard scale related to spontaneous chiral symmetry breaking. The pion and pion-nucleon sectors are perturbative in Q, the corresponding EFT is the chiral perturbation theory (CHPT). The parameters in $\mathcal{L}_{\pi\pi}$ and $\mathcal{L}_{\pi{\rm N}}$ are known from CHPT studies, these are the so-called low-energy constants (LECs). Matters are more difficult/interesting for systems with two or more nucleons. The small nuclear binding energies (or large S-wave scattering lengths) require a non-perturbative resummation to have a useful approach up

[a] e-mail: meissner@itkp.uni-bonn.de

to the pion production threshold. Following Weinberg [2], the organization of the theory takes place on the level of the effective potential $V_{\rm eff}$ which is then injected into a regularized Lippmann-Schwinger equation to generate the bound and scattering states. The various terms in the effective potential are ordered according to

$$V_{\rm eff} \equiv V_{\rm eff}(Q,g,\mu) = \sum_\nu Q^\nu \, \mathcal{V}_\nu(Q/\mu, g)\,, \qquad (3)$$

where Q is the soft scale (either a baryon three-momentum, a Goldstone boson four-momentum or a Goldstone boson mass), g is a generic symbol for the pertinent low-energy constants, μ a regularization scale, $\mathcal{V}_\nu$ is a function of order one (naturalness), and $\nu \geq 0$ is the chiral power. It can be expressed as (for connected diagrams)

$$\nu = 2 - B + 2L + \sum_i v_i \, \Delta_i\,, \quad \Delta_i = d_i + \frac{1}{2}\, b_i - 2\,, \quad (4)$$

with B the number of incoming (outgoing) baryon fields, L counts the number of Goldstone boson loops, and v_i is the number of vertices with dimension Δ_i. The vertex dimension is expressed in terms of derivatives (or Goldstone boson masses) d_i and the number of internal baryon fields b_i at the vertex under consideration. The leading-order (LO) potential is given by $\nu = 0$, with $B = 2$, $L = 0$ and $\Delta_i = 0$. Using eq. (4) it is easy to see that this latter condition is fulfilled for two types of interactions: a) non-derivative four-baryon contact terms with $b_i = 4$ and $d_i = 0$ and b) one-meson exchange diagrams with the leading meson-baryon derivative vertices allowed by chiral symmetry ($b_i = 2, d_i = 1$). At next-to-leading order (NLO), one encounters the first contribution from two-pion exchange and so on. Also, three- (four-) nucleon forces first appear at NN(N)LO. This parametrical suppression explains naturally the observed hierarchy of nuclear forces. The potential requires further regularization when injected into the Lippmann-Schwinger equation, here the so-called spectral function regularization has become the method of choice to further separate the short- and the long-distance physics (for details, see [3]). For further details on nuclear EFT, I refer to the recent and comprehensive review by Epelbaum [4].

3 The forces between two nucleons

The two-nucleon forces have been analyzed to a high precision, more precisely to N^{3}LO [5,6]. The one- and two-pion exchanges are given in terms of LECs from the pion-nucleon Lagrangian, these have been previously determined in studies of pion-nucleon scattering and pion production in pion-nucleon collisions (for an update on the dimension two LECs, see [7] and some of the third-order LECs were determined in refs. [8,9]). Three-pion exchange also appears at N^{3}LO, but it has been shown to contribute negligibly [10]. This information from πN scattering constitutes the direct link to QCD via its symmetries and their realizations. The four-nucleon couplings must

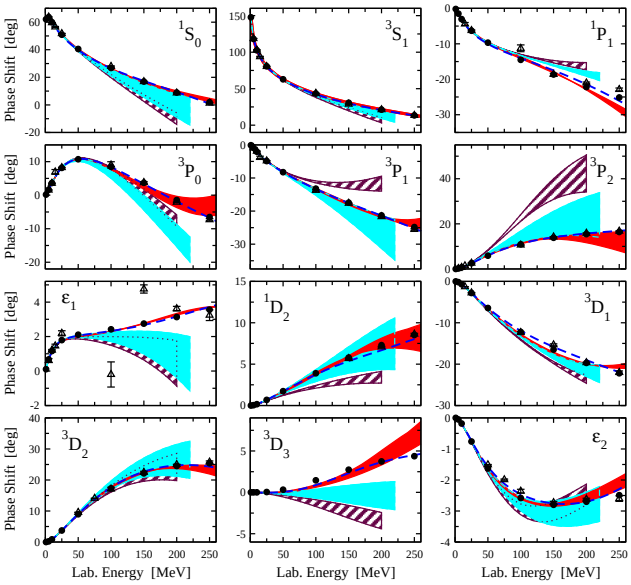

Fig. 1. Low np phase shifts as a function of the nucleon laboratory energy. The hatched, light-shaded, and dark-shaded bands denote the NLO, NNLO and N^{3}LO results, respectively. The N^{3}LO results from ref. [5] are shown by the dashed lines. Also shown are the results from the Nijmegen [11] (filled circles) and the Virginia Tech [12] (open triangles) partial-wave analyses.

be determined from a fit to the low NN phases (obtained, *e.g.*, from the Nijmegen partial-wave analysis). At LO, N(N)LO and N^{3}LO, there are 2, 7, and 15 four-nucleon independent couplings (note that at NNLO one has no new contact terms due to parity). In addition, one has to account for the effects of electromagnetism and other strong isospin breaking effects in the pp, np and nn channels. This machinery has also been developed in the past years, see *e.g.* the review [4]. The resulting description of the S-, P- and D-waves of np scattering at NLO, NNLO and N^{3}LO is shown in fig. 1. As expected for a converging EFT, the theoretical uncertainty decreases with increasing order. The description of the low phases is excellent and the resulting S-wave scattering lengths and effective range parameters are in good agreement with the ones obtained from the Nijmegen PWA. Also, the deuteron properties are well reproduced. For any practical application, the EFT description of the two-nucleon system now matches the accuracy of the so-called high-precision (semi)phenomenological potentials —quite a milestone for the EFT program for nuclear physics. What remains to be done is the consistent construction of the electroweak currents —work along these lines is in progress.

4 Three-nucleon forces

One of the most appealing features of the EFT approach is the consistent derivation of two- and three-nucleon forces —this was simply not possible in the conventional approach based on meson-exchanges and alike. The leading

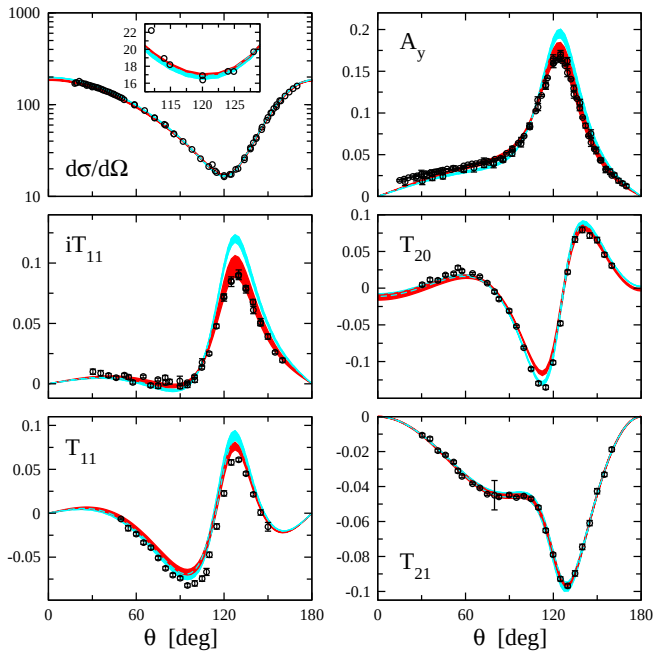

Fig. 2. *nd* elastic scattering observables (differential cross-section, vector and tensor analyzing powers) at 10 MeV at NLO (light-shaded bands) and at NNLO (dark-shaded bands). Note that at NLO, the 3NF is still absent. The data can be traced back from ref. [14].

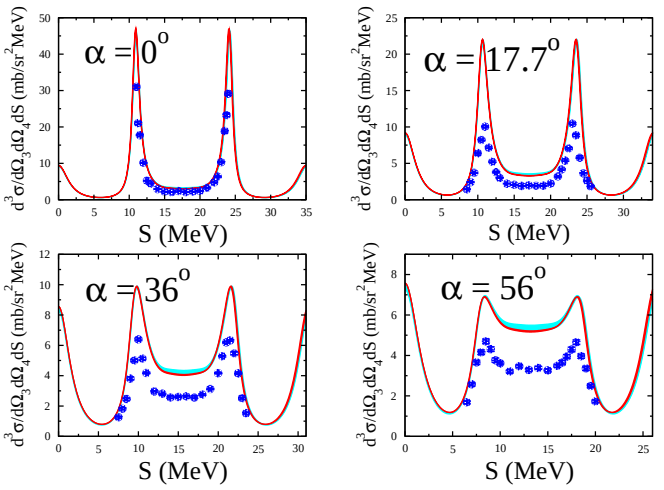

Fig. 3. Differential cross-section for *pd* break-up in the symmetric constant relative energy configuration at $E_d = 19$ MeV for $\alpha = 0°, 17.7°, 36°$ and $56°$ compared to the NNLO calculation.

3NF appears at NNLO and is given in terms of three topologies. These are the tree level two-pion exchange, the one-pion exchange (between a 4N contact term and the third nucleon) and a genuine 6N contact interaction. While the LECs related to the TPE topology are known from πN scattering, the other two contributions contain one unknown LEC, respectively. These LECs are called c_D and c_E, respectively. As already discussed some time ago, the second topology also features in pion production in *pp* collisions [13], this again shows the strength of EFT connecting many different processes and reactions. To pin down the LECs, one has to use two low-energy input data. In ref. [14], the triton binding energy and the doublet *nd* scattering length $^2a_{nd}$ were used to determine c_E and c_D. An update is given in the review [4] and a study of the 3NF in ^{7}Li in the framework of the no-core shell model was presented in [15]. Already at this order in the chiral expansion, one obtains an excellent description of many *pd* and *nd* scattering and break-up data, see, *e.g.*, fig. 2.

However, there are various good reasons to work out the 3NF at N^{3}LO. First, of course, one wants to achieve consistency with the two-nucleon force which is already available at N^{3}LO (see above). Second if one considers the same observables as in fig. 2 for higher energies, *e.g.* for $E_n = 65$ MeV, the theoretical uncertainty is uncomfortably large. Third, at very low energies there are still discrepancies in the description of the vector analyzing power A_y and also, recent measurements at Cologne [16] of *pd* break-up in the "symmetric relative constant energy" configuration at $E_d = 19$ MeV show significant deviations from the NNLO prediction with increasing angle α (the angle between the space-star configuration of the three outgoing nucleons and the incoming deuteron), see fig. 3. Note that the also measured analyzing powers A_{yy} agree much better with the theoretical predictions, for details see [16]. Thus, it is mandatory to calculate the 3NF at N^{3}LO. This is quite a formidable task, but work in progress by Bernard, Epelbaum and others looks very promising. Furthermore, recent progress in the inclusion of Coulomb effects in three-nucleon systems [17] has to be built into the EFT. It is also worth mentioning that the 4NF, that first appears at N^{4}LO, has recently been presented by Epelbaum [18]. For a first estimate of the effects of this force in ^{4}He, see [19].

5 Hyperon-nucleon forces

Strange quark effects in nuclei are investigated in the field of hyper-nuclear physics. To address such issues requires the knowledge of the fundamental hyperon-nucleon (YN) interactions. Before discussing these in the framework of a chiral EFT, let me stress the differences to the NN case. First, there exist not many data for low and moderate energies and also, their precision is mostly limited. A partial-wave analysis is therefore not available. However, the ambitious hyper-nuclear programs at KEK, CEBAF, MAMI, DAΦNE and JPARC will provide further specific information on the YN interaction by mapping out precisely the level schemes of a large variety of hyper-nuclei. Second, one has to consider channel coupling in the physical basis due to the Λ-Σ^0 mixing. Third, due to the larger strange quark mass, bigger explicit chiral symmetry-breaking effects are expected.

In ref. [20], we have considered the YN interaction in chiral effective field theory to leading order in the power counting, cf. eq. (4) (for an earlier analysis treating the

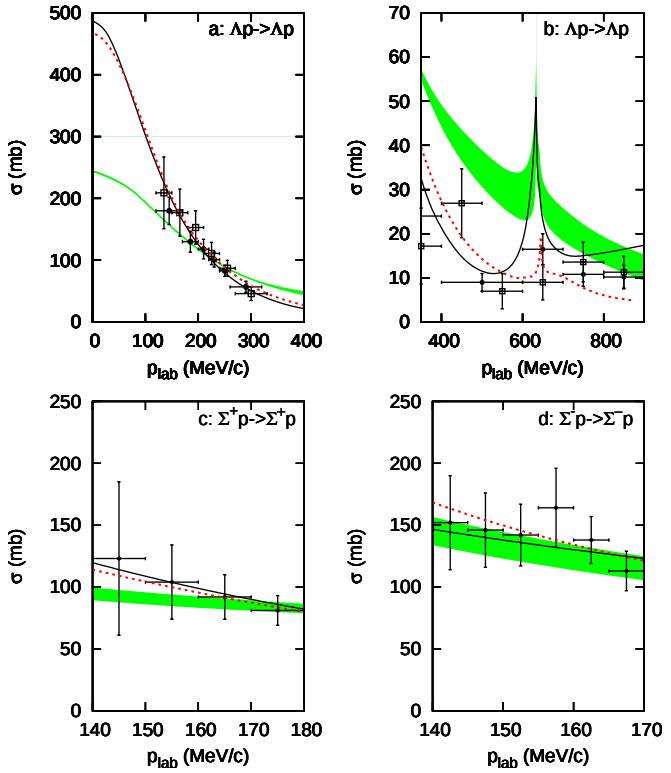

Fig. 4. "Total" cross-section σ (as defined in eq. (9)) as a function of $p_{\rm lab}$. The shaded band is the chiral EFT potential for $\Lambda = 550, \ldots, 700$ MeV, the dashed curve is the Jülich '04 model [23], and the solid curve is the Nijmegen NSC97f model [24].

boson exchanges perturbatively, see [21]). Such an exploratory study is motivated by the fact that a) in the YN system the S-wave scattering lengths (that are not precisely known) are not as unnaturally large as in the NN sector and b) the three-flavor theory is much richer at leading order. More precisely, we have to consider the contact interactions of the baryon octet,

$$B = \begin{pmatrix} \frac{\Sigma^0}{\sqrt{2}} + \frac{\Lambda}{\sqrt{6}} & \Sigma^+ & p \\ \Sigma^- & \frac{-\Sigma^0}{\sqrt{2}} + \frac{\Lambda}{\sqrt{6}} & n \\ -\Xi^- & \Xi^0 & -\frac{2\Lambda}{\sqrt{6}} \end{pmatrix} . \tag{5}$$

Here, we identify the physical η with the octet particle —this is correct modulo NLO corrections. It is shown in ref. [20] that there are 6 independent four-baryon contact terms without derivatives, from which 5 combinations appear in the YN system (the sixth combination only contributes to the $\Lambda\Lambda$ and ΞN channels). Thus, one has to determine the 5 corresponding LECs. This is done best in the partial-wave basis:

$$\begin{aligned} V^{\Lambda\Lambda}_{1S0} &= C^{\Lambda\Lambda}_{1S0}\,, \quad V^{\Lambda\Lambda}_{3S1} = C^{\Lambda\Lambda}_{3S1}\,, \\ V^{\Sigma\Sigma}_{1S0} &= C^{\Sigma\Sigma}_{1S0}\,, \quad V^{\Sigma\Sigma}_{3S1} = C^{\Sigma\Sigma}_{3S1}\,, \\ \widetilde{V}^{\Sigma\Sigma}_{1S0} &= 9C^{\Lambda\Lambda}_{1S0} - 8C^{\Sigma\Sigma}_{1S0}\,, \quad \widetilde{V}^{\Sigma\Sigma}_{3S1} = C^{\Lambda\Lambda}_{3S1}\,, \\ V^{\Lambda\Sigma}_{1S0} &= 3\left(C^{\Lambda\Lambda}_{1S0} - C^{\Sigma\Sigma}_{1S0}\right)\,, \quad V^{\Lambda\Sigma}_{3S1} = C^{\Lambda\Sigma}_{3S1}\,, \end{aligned} \tag{6}$$

that features singlet and triplet waves (supplemented by appropriate isospin factors),

$$V^{(0)} = C^{BB}_S + C^{BB}_T\ \boldsymbol{\sigma}_1 \cdot \boldsymbol{\sigma}_2\,. \tag{7}$$

In [20], we have chosen to search for $C^{\Lambda\Lambda}_{1S0}$, $C^{\Lambda\Lambda}_{3S1}$, $C^{\Sigma\Sigma}_{1S0}$, $C^{\Sigma\Sigma}_{1S0}$, and $C^{\Lambda\Sigma}_{3S1}$ in the fitting procedure. The other three partial-wave potentials are then determined by $SU(3)$-symmetry. In addition, there is the leading one-Goldstone-boson exchange from the pseudoscalar octet (π, K, η)

$$\mathcal{L} = \left\langle \frac{D}{2}\bar{B}\gamma^\mu\gamma_5\,\{u_\mu, B\} + \frac{F}{2}\bar{B}\gamma^\mu\gamma_5\,[u_\mu, B] \right\rangle\,, \tag{8}$$

where the brackets denote the trace in flavor space. In the $SU(3)$ limit (that is to LO), all baryon-meson couplings can be expressed in terms of the pion-nucleon coupling f and the $SU(3)$ ratio $\alpha = D/(D+F)$, subject to the constraint that $F + D = g_A$, with g_A the nucleon axial-vector coupling. We use $\alpha = 0.4$ but also have performed fits for α in the range $[0.36, 0.44]$. Symmetry breaking in the meson decay constants only appears at NLO. Note that we also have performed calculations neglecting η exchange, as it is often done in meson-exchange models. The fits are not very sensitive to this, but it is remarkable that the consistent inclusion of the eta leads to a somewhat improved plateau (that is a smaller variation of the χ^2/dof as the cut-off in the LS equation is varied). We also include the leading Coulomb effects using the Vincent-Phatak procedure properly formulated for the EFT, see, *e.g.*, ref. [22]. Altogether, we fit to 34 total cross-section data points and the $\Sigma^- p$ capture ratio at rest. The total cross-sections are found by simply integrating the differential cross-sections, except for the $\Sigma^+ p \to \Sigma^+ p$ and $\Sigma^- p \to \Sigma^- p$ channels. For those channels the experimental total cross-sections were obtained via

$$\sigma = \frac{2}{\cos\theta_{\rm max} - \cos\theta_{\rm min}} \int_{\cos\theta_{\rm min}}^{\cos\theta_{\rm max}} \frac{{\rm d}\sigma(\theta)}{{\rm d}\cos\theta}{\rm d}\cos\theta\,, \tag{9}$$

for various values of $\cos\theta_{\rm min}$ and $\cos\theta_{\rm max}$. Following [24], we use $\cos\theta_{\rm min} = -0.5$ and $\cos\theta_{\rm max} = 0.5$ in our calculations for the $\Sigma^+ p \to \Sigma^+ p$ and $\Sigma^- p \to \Sigma^- p$ cross-sections, in order to stay as close as possible to the experimental procedure. We also impose the constraint that the fits should produce a bound hyper-triton with roughly the correct binding energy. For a reasonable cut-off variation, the four-baryon LECs come out of natural size,

$$\begin{aligned} 4\pi\, m_B^2\, C^{\Lambda\Lambda}_{1S0} &= -0.6, \ldots, -0.4\,, \\ 4\pi\, m_B^2\, C^{\Lambda\Lambda}_{3S1} &= -0.3, \ldots, -0.03\,, \\ 4\pi\, m_B^2\, C^{\Sigma\Sigma}_{1S0} &= -1.1, \ldots, -1.0\,, \\ 4\pi\, m_B^2\, C^{\Sigma\Sigma}_{3S1} &= 3.2, \ldots, 3.5\,, \\ 4\pi\, m_B^2\, C^{\Lambda\Sigma}_{3S1} &= -0.1, \ldots, 0.05\,, \end{aligned} \tag{10}$$

with $m_B \simeq 1.1$ GeV the average octet baryon mass, and the corresponding description of the total cross-sections for some of the channels is shown in fig. 4. The shaded band is obtained by varying the cut-off in the Lippmann-Schwinger equation between 550 and 700 MeV, the corresponding total χ^2 varies from 29.6 to 34.6. The resulting

Table 1. The YN singlet and triplet scattering lengths (a) and effective ranges (r) (in fm) and the hyper-triton binding energy, E_B (in MeV) as a function of the cut-off Λ (in MeV). The binding energies for the hyper-triton (last row) are calculated using the Idaho-N^{3}LO NN potential [5]. The experimental value of the hyper-triton binding energy is $-2.354(50)$ MeV.

Λ	550	600	650	700
$a_S^{\Lambda p}$	-1.90	-1.91	-1.91	-1.91
$r_S^{\Lambda p}$	1.40	1.40	1.36	1.35
$a_T^{\Lambda p}$	-1.22	-1.23	-1.23	-1.23
$r_T^{\Lambda p}$	2.05	2.13	2.20	2.27
$a_S^{\Sigma^+ p}$	-2.24	-2.32	-2.36	-2.39
$r_S^{\Sigma^+ p}$	3.74	3.60	3.53	3.63
$a_T^{\Sigma^+ p}$	0.70	0.65	0.60	0.56
$r_T^{\Sigma^+ p}$	-2.14	-2.78	-3.55	-4.36
E_B	-2.35	-2.34	-2.34	-2.36

singlet and triplet scattering lengths, the effective ranges and the corresponding hyper-triton binding energy are collected in table 1. Note that a Λp singlet scattering lengths of about -1.9 fm leads to the correct hyper-triton binding energy (within 0.5% of the empirical value). This value for $a_S^{\Lambda p}$ differs considerably from the one obtained in meson-exchange models [23,25].

Our findings show that the chiral effective field theory scheme, applied earlier to the NN interaction, also works well for the YN interaction. In the future it will be interesting to study the convergence of the chiral EFT for the YN interaction by doing NLO and NNLO calculations. In view of hyper-nucleus calculations, three-baryon forces that naturally arise in chiral EFT, should be investigated too (for a study of the hyper-triton in an EFT with contact interactions, see [26]). Furthermore, a combined NN and YN study in chiral EFT, starting with a NLO calculation, needs to be performed. Work in this direction is in progress.

6 Pion production in proton-proton collisions

As noted before, (threshold) pion production in proton-proton collisions encodes further complementary information on the structure of the few-nucleon forces. Also, there exist a waste amount of precise data for the reactions $pp \to pp\pi^0, pp \to d\pi^+, \ldots$ from COSY at Jülich, IUCF at Bloomington, TRIUMF at Vancouver and from TSL at Uppsala, for a recent and comprehensive review see [27]. These reactions are characterized by a fairly large momentum transfer squared already at threshold:

$$t \simeq -m_{\rm N} M_\pi = -(360\,{\rm MeV})^2\,. \qquad (11)$$

Consequently, the power counting has to be adjusted correspondingly, the appropriate expansion parameter is $\chi = \sqrt{M_\pi/m_{\rm N}} \simeq 0.4$. It was already demonstrated in ref. [28] that such a power counting leads to the correct ordering of the various contributions at threshold (which had earlier been evaluated in the standard Weinberg counting with some rather strange findings, see *e.g.* [29]). Furthermore, in contrast to the construction of 2N and 3N forces, in pion production one must include the $\Delta(1232)$-resonance explicitely in the EFT. Another important issue, which was only understood recently [30], is the way one has to consistently include the initial-state and the final-state interactions together with the interaction kernel —otherwise one is left with amplitudes that cannot be controlled by analytic contributions. In [30] we have performed a NLO calculation of the threshold cross-section $\sigma_{\rm thr}$ for $pp \to d\pi^+$ incorporating all these ingredients. In the threshold region, the cross-section can be written as

$$\sigma_{\rm thr} = \alpha\eta + \beta\eta^3 + \mathcal{O}(\eta^5)\,, \quad \eta = p_\pi/M_\pi\,. \qquad (12)$$

The leading-order calculation leads to a too small cross-section by about a factor of 2/3, $\alpha^{\rm LO} = 131\,\mu$b, see the dashed line in fig. 5. At NLO, this factor is effectively recovered, without any adjustable parameter one finds (for details, see [30])

$$\alpha^{\rm NLO} = 220\,\mu{\rm b}\,, \qquad (13)$$

as shown by the solid line in fig. 5. However, at this order one still has a sizeable uncertainty, which is depicted by the grey hatched area in the figure. Needless to say that much work needs to be done to sharpen these conclusions, in particular, the NNLO corrections, which contain for the first time counter terms, have to be worked out. Also, the intricate reaction $pp \to pp\pi^0$, that is sensitive to the small isoscalar pion-nucleon scattering amplitude, can now be addressed systematically.

Let me point out that the NNπ intermediate state plays an important role in the calculation of the dispersive and absorptive corrections to the complex-valued pion-deuteron scattering length. In ref. [31] a parameter-free

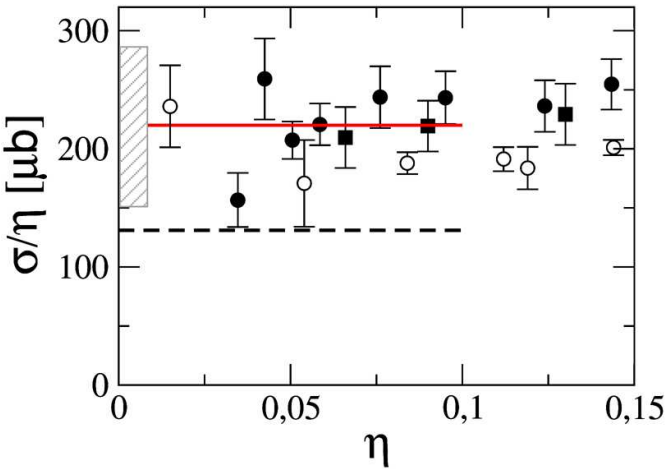

Fig. 5. Comparison of the NLO results to experimental data for $pp \to d\pi^+$. The dashed and the solid curves show the LO and the NLO result, respectively. The grey hatched area depicts the theoretical uncertainty at NLO. The data can be traced back from ref. [30].

calculation of these corrections based on chiral perturbation theory is presented. It is shown that once *all* diagrams contributing to leading order to this process are included, their net effect provides a small correction to the real part of the pion-deuteron scattering length. At the same time the sizable imaginary part of the pion-deuteron scattering length is reproduced accurately.

7 Summary and outlook

In this talk, I have presented the foundations and various applications of the modern theory of nuclear forces. It has a direct relation to QCD via its symmetries (and their realizations) and is a systematic and precise approach based on the chiral effective Lagrangian of pions, nucleons and external sources. In this framework, it is possible to derive three-nucleon forces (see sect. 4) and external electroweak currents that are consistent with the dominant NN forces. Furthermore, utilizing again the effective chiral Lagrangian, one can derive consistently nucleon and nuclear properties, which is of particular importance for the model-independent extraction of neutron properties from light nuclear targets such as deuterium or ^{3}He. As discussed in sect. 5, the extension of this scheme to include strange quarks, more precisely the exploratory study for the hyperon-nucleon interactions, look quite promising. Chiral effective-field theory also allows for a variation of the fundamental QCD parameters, like *e.g.* the quark masses, and thus provides chiral extrapolation functions for the analysis of lattice QCD sector (for a status report on these activities, see [32]).

Clearly, there is lots of work ahead to make further progress:

a) the three-nucleon forces should be worked out to N^{3}LO,
b) the electroweak current operators have to be constructed to N^{3}LO,
c) further systematic studies of pion production in proton-proton collisions at NNLO are to be carried out,
d) a combined analysis of NN and YN interactions at (N)NLO would certainly shed further light on the details of the YN interactions, and
e) more work should also be devoted to extend this scheme to medium and heavy nuclei (halos, cluster structures, no-core shell model, ...), which will be of importance for the nuclear-structure program at the future FAIR facility and other radioactive-beam facilities world-wide.

In summary, let me say that a new era of nuclear physics has just begun.

I am grateful to all my collaborators from Bonn, Jülich, Strasbourg, ... for very pleasant collaborations on the topics reported here. I also thank Evgeny Epelbaum for a careful reading of the manuscript. This work is supported in parts by the EU Integrated Infrastructure Initiative Hadron Physics Project under contract number RII3-CT-2004-506078 and by DFG (SFB/TR 16, "Subnuclear Structure of Matter").

References

1. S. Pieper, Nucl. Phys. A **751**, 516 (2005).
2. S. Weinberg, Nucl. Phys. B **363**, 3 (1991).
3. E. Epelbaum, W. Glöckle, U.-G. Meißner, Eur. Phys. J. A **19**, 125 [nucl-th/0304037]; 401 [nucl-th/0308010] (2004).
4. E. Epelbaum, Prog. Part. Nucl. Phys. **57**, 654 (2006) [arXiv:nucl-th/0509032].
5. D.R. Entem, R. Machleidt, Phys. Rev. C **68**, 041001 (2003) [arXiv:nucl-th/0304018].
6. E. Epelbaum, W. Glöckle, U.-G. Meißner, Nucl. Phys. A **747**, 362 (2005) [arXiv:nucl-th/0405048].
7. U.-G. Meißner, PoS (LAT2005) 009 [arXiv:hep-lat/0509029].
8. N. Fettes, U.-G. Meißner, Nucl. Phys. A **676**, 311 (2000) [arXiv:hep-ph/0002162].
9. N. Fettes, U.-G. Meißner, Nucl. Phys. A **693**, 693 (2001) [arXiv:hep-ph/0101030].
10. N. Kaiser, Phys. Rev. C **61**, 014003 (2000) [arXiv:nucl-th/9910044]; **62**, 024001 (2000) [arXiv:nucl-th/9912054].
11. V.G.J. Stoks *et al.*, Phys. Rev. C **48**, 792 (1993).
12. SAID on-line program, `http://gwdac.phys.gw.edu`.
13. C. Hanhart, U. van Kolck, G.A. Miller, Phys. Rev. Lett. **85**, 2905 (2000) [arXiv:nucl-th/0004033].
14. E. Epelbaum, A. Nogga, W. Glöckle, H. Kamada, U.-G. Meißner, H. Witala, Phys. Rev. C **66**, 064001 (2002) [arXiv:nucl-th/0208023].
15. A. Nogga, P. Navratil, B.R. Barrett, J.P. Vary, Phys. Rev. C **73**, 064002 (2006) [arXiv:nucl-th/0511082].
16. J. Ley *et al.*, Phys. Rev. C **73**, 064001 (2006).
17. A. Deltuva, A.C. Fonseca, P.U. Sauer, Phys. Rev. C **71**, 054005 (2005) [arXiv:nucl-th/0503012].
18. E. Epelbaum, Phys. Lett. B **639**, 456 (2006) [arXiv:nucl-th/0511025].
19. D. Rozpedzik *et al.*, arXiv:nucl-th/0606017.
20. H. Polinder, J. Haidenbauer, U.-G. Meißner, Nucl. Phys. A **779**, 244 (2006) [arXiv:nucl-th/0605050].
21. C.L. Korpa, A.E.L. Dieperink, R.G.E. Timmermans, Phys. Rev. C **65**, 015208 (2002) [arXiv:nucl-th/0109072].
22. M. Walzl, U.-G. Meißner, E. Epelbaum, Nucl. Phys. A **693**, 663 (2001) [arXiv:nucl-th/0010019].
23. J. Haidenbauer, U.-G. Meißner, Phys. Rev. C **72**, 044005 (2005) [arXiv:nucl-th/0506019].
24. Th.A. Rijken, V.G.J. Stoks, Y. Yamamoto, Phys. Rev. C **59**, 21 (1999).
25. T.A. Rijken, Y. Yamamoto, Phys. Rev. C **73**, 044008 (2006) [nucl-th/0603042].
26. H.W. Hammer, Nucl. Phys. A **705**, 173 (2002) [arXiv:nucl-th/0110031].
27. C. Hanhart, Phys. Rep. **397**, 155 (2004) [arXiv:hep-ph/0311341].
28. C. Hanhart, N. Kaiser, Phys. Rev. C **66**, 054005 (2002) [nucl-th/0208050].
29. B.Y. Park, F. Myhrer, J.R. Morones, T. Meissner, K. Kubodera, Phys. Rev. C **53**, 1519 (1996) [arXiv:nucl-th/9512023].
30. V. Lensky, V. Baru, J. Haidenbauer, C. Hanhart, A.E. Kudryavtsev, U.-G. Meißner, Eur. Phys. J. A **27**, 37 (2006) [arXiv:nucl-th/0511054].
31. V. Lensky, V. Baru, J. Haidenbauer, C. Hanhart, A. Kudryavtsev, U.-G. Meißner, arXiv:nucl-th/0608042; to be published in Phys. Lett. B (2007).
32. M.J. Savage, arXiv:nucl-th/0601001.